

Application of scaled boundary finite element method on soil-structure interaction – two dimensions dynamic coupled consolidation analysis of fully saturated soils

Mahmoud Hassanen
Department of Civil Engineering
Strathclyde University
Glasgow, G4 0NG
United Kingdom

Abstract: - The scaled boundary finite element method (SBFEM) combines the advantages of finite element method (FEM) and boundary element method (BEM). Therefore, it is considered as a powerful tool to analyse the soil-structure interaction problems. In this research, this method is extended to include Biot's coupled consolidation in order to deal with fully saturated soil as two-phase medium. The general 2D dynamic analysis case, including body forces and surface tractions in different media in the frequency domain, is formulated. In addition, Chebyshev pseudospectral method is introduced for solving the FE coupled consolidation equations.

Key-Words: - SBFEM, Frequency domain, Soil-structure interaction, Biot, Coupled consolidation

1 Introduction

As you can see for the title of the paper you must The scaled boundary finite element method (SBFEM) is essentially a semi-analytical technique developed recently by Wolf and Song ([1]-[6]). The SBFEM combines the advantages of finite element method (FEM) and boundary element method (BEM). In particular, it discretises boundaries only so that the modelled spatial dimensions are reduced by one as the BEM and meanwhile it does not need fundamental solution as the FEM [7]. Therefore, the wide applicability of the FEM and the simplicity in remeshing of the BEM can be potentially retained. Moreover, The SBFEM has superior ability to handle problems with singularities and discontinuities over other conventional numerical methods as recently reported by Li et. al. [8, 9].

In addition, a virtual work derivation for elastostatics [10] increased the transparency of the method considerably, leading to the development of stress recovery and error estimation procedures [11], which in turn allowed adaptive procedures to be implemented [12]. On using these procedures, direct comparison of computational cost for achievement of a prescribed level of accuracy was possible, and the method was shown to be more efficient than the finite element method for problems involving unbounded domains and for problems involving stress singularities or discontinuities.

Wolf [13] presented a comprehensive review of the method and presented many examples.

SBFEM has been used to solve the two-dimensional Laplace's equation for potential flow around obstacles by Deeks and Cheng [14]. They found that SBFEM was capable of resolving the velocity singularity at corners of a rectangular cylinder with a very coarse mesh. In addition, they demonstrated that a significant number of grid points is needed to resolve the same velocity singularity using finite difference method. Further, Li et al. [8, 9] developed a solution of two dimensional Helmholtz equations for wave diffraction by a vertical bottom-mounted cylinder and analyzed the interactions of multiple cylinders with a substructuring technique. Li et al. [15, 16] extend the original SBFEM to solve the problems with a band-shaped infinite domain with infinitely long parallel boundaries to solve problems of wave diffraction around a fixed single obstacle and twin obstacles and wave radiation around floating structures oscillating in water of finite depth. The SBFEM is also applied to analysis of wave propagation in solid materials under moving loads [17] and to model mixed-mode automatic crack propagation in brittle or quasi-brittle materials based on the linear elastic fracture mechanics [7].

Due to its distinct features, the SBFEM has attracted considerable attention in modelling structural and soil-structure interaction problems [13, 18]. In

particular, the SBFEM has been shown to outperform the traditional finite-element method in terms of both accuracy and computational efficiency for elasto-static [10], elasto-dynamic ([11, 12]) and elasto-plastic unbounded media [19]. In addition, incompressibility, body loads (self-weight) and elastic anisotropy can be handled with ease [18], and diffusion problems, such as pore water pressure in a drained soil analysis, can also be modelled ([4], [14]). Extension to unbounded domains in which the material properties vary with depth [20] and to axisymmetric geometries with general loading [21] allowed fruitful application of the method to many foundation problems [22].

In this paper, the SBFEM has been extended to include Biot's coupled consolidation in order to deal with fully saturated soil as a two-phase medium. In particular, the numerical formulation that considers the general 2D analysis case is developed, accounting for body forces and surface tractions in both bounded and unbounded media in the frequency domain. In addition, the formulation is capable of correctly modelling the dynamic far-field boundary condition for two-phase media, and studies its effect on the time-dependent interaction between a structure, and the underlying local soil.

2 Governing Equations

The Biot's coupled consolidation equations [23] comprise a system of simultaneous differential equations which satisfy; (a) the equilibrium conditions (the dynamic equations of motion) and (b) the continuity equations. The 2D form of these equations in the frequency domain is shown as equations (1a) and (1b).

$$[L]^T (\{\sigma'\} + \{m\}p) + \omega^2 \rho \{u\} + \rho \{b\} = 0 \quad (1a)$$

$$\begin{aligned} & -k\{m\}^T [L][L]^T \{m\}p \\ & + \omega^2 k \rho_f \{m\}^T [L]\{u\} \\ & + k \rho_f \{m\}^T [L]\{b\} \end{aligned} \quad (1b)$$

$$+ i\omega \{m\}^T [L]\{u\} + i\omega \frac{n}{K_f} p = 0$$

The differential operator $[L]$ is defined by equation (2) σ' is the effective stress, p is the fluid pressure (in which the total stress σ relates to the fluid pressure by $\{\sigma\} = \{\sigma'\} + \{m\}p$, u , ω , k , n , k_f

and ρ are the displacement, frequency, soil permeability and porosity, fluid bulk modulus and density respectively, and $\{b\}$ is a vector representing the body forces per unit volume.

$$[L] = \begin{bmatrix} \partial/\partial x & 0 \\ 0 & \partial/\partial y \\ \partial/\partial y & \partial/\partial x \end{bmatrix} \quad (2)$$

3 Scaled Boundary Transformation of Geometry

Consider a finite line element 1-2 forming the base of the triangle shown in Fig. 1. Any point A on the boundary line element 1-2, with local coordinates (x, y) can be represented by its position vector r , where $r = x\hat{i} + y\hat{j}$. If the origin, O , of the Cartesian coordinates (\hat{x}, \hat{y}) coincides with the apex of the triangle, then a point within the domain may be described in the Cartesian coordinates by its global position vector \hat{r} as $\hat{r} = \hat{x}\hat{i} + \hat{y}\hat{j}$. To transfer from the Cartesian to the curvilinear co-ordinate system (ξ, η) , any point within the domain (in which $\xi = 1$ at the boundary and $\xi = 0$ at the scaling centre) may be described by scaling using the position vector of the corresponding boundary point; $\hat{r} = \xi r$. Fig. 1 shows the geometry of the line boundary with the tangential vector (slope) in the η direction, represented by the derivative of the point A's position vector on the line as shown in equation (3):

$$r_{,\eta} = x_{,\eta}\hat{i} + y_{,\eta}\hat{j} \quad (3)$$

Mathematically, the geometry of the boundary of the finite element shown in Fig. 1 may be represented by interpolating its nodal coordinates $\{x\}$ and $\{y\}$ using the local coordinates η at the boundary as follows

$$\begin{aligned} x(\eta) &= [N(\eta)]\{x\} = [N]\{x\} \\ \text{and } y(\eta) &= [N(\eta)]\{y\} = [N]\{y\} \end{aligned} \quad (4)$$

Where

$$\begin{aligned} [N] &= [N(\eta, \zeta)] \\ &= [N_1(\eta, \zeta) \quad N_2(\eta, \zeta) \quad \dots \quad N_n(\eta, \zeta)] \\ &= [N_1 \quad N_2 \quad \dots \quad N_n] \end{aligned}$$

and n is the number of element nodes. Using the scaling relationship $\hat{\mathbf{r}} = \xi \mathbf{r}$ to describe the position of any point within the domain leads to

$$\hat{x}(\xi, \eta) = \xi x(\eta) \text{ and } \hat{y}(\xi, \eta) = \xi y(\eta) \quad (5)$$

Equation (6) is used to transfer the differential operators in the (\hat{x}, \hat{y}) co-ordinate system to those corresponding to the (ξ, η) co-ordinate system

$$\begin{aligned} \begin{Bmatrix} \partial/\partial\hat{x} \\ \partial/\partial\hat{y} \end{Bmatrix} &= [\hat{\mathbf{J}}(\xi, \eta)]^{-1} \begin{Bmatrix} \partial/\partial\xi \\ \partial/\partial\eta \end{Bmatrix} \\ &= \frac{1}{|\mathbf{J}|} \begin{bmatrix} y_{,\eta} & -x_{,\eta} \\ -y & x \end{bmatrix} \begin{Bmatrix} \partial/\partial\xi \\ \partial/\partial\eta \end{Bmatrix} \end{aligned} \quad (6)$$

where the Jacobian matrix is

$$[\hat{\mathbf{J}}(\xi, \eta)] = \begin{bmatrix} \hat{x}_{,\xi} & \hat{y}_{,\xi} \\ \hat{x}_{,\eta} & \hat{y}_{,\eta} \end{bmatrix}$$

and the determinant is $|\mathbf{J}| = xy_{,\eta} - yx_{,\eta}$

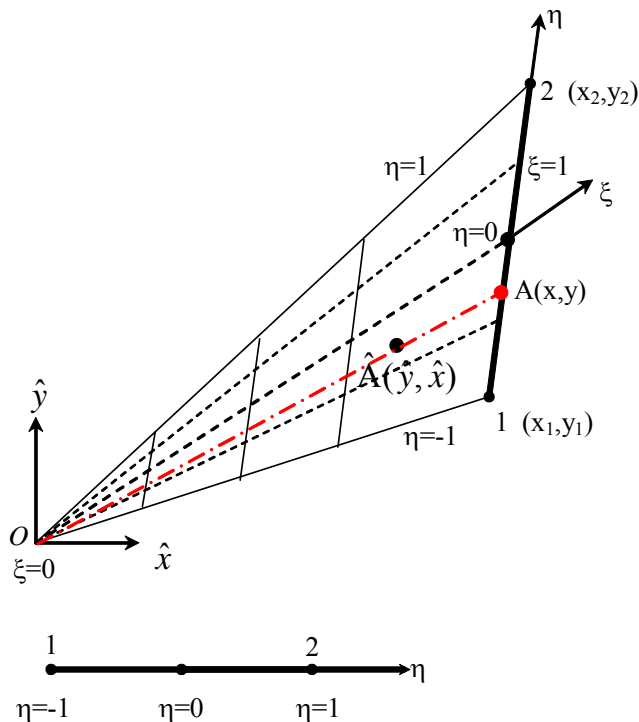


Fig. 1. Scaled boundary transformation of geometry of line finite element.

At $\xi = 1$, on the element boundary, the outward normal vector is defined by equation (7).

$$\mathbf{g}^\xi = \mathbf{r}_{,\eta} = y_{,\eta} \mathbf{i} - x_{,\eta} \mathbf{j} \quad (7a)$$

The unit normal vector, \mathbf{n}^ξ is thus

$$\mathbf{n}^\xi = \frac{\mathbf{g}^\xi}{g^\xi} = n_x^\xi \mathbf{i} + n_y^\xi \mathbf{j} = \frac{1}{g^\xi} [y_{,\eta} \mathbf{i} - x_{,\eta} \mathbf{j}] \quad (7b)$$

Similarly, the outward normal vector to the line (ξ) is \mathbf{g}^η : $\mathbf{g}^\eta = \mathbf{r} = -y \mathbf{i} + x \mathbf{j}$ (8a)

and the corresponding unit normal vector is \mathbf{n}^η .

$$\mathbf{n}^\eta = \frac{\mathbf{g}^\eta}{g^\eta} = n_x^\eta \mathbf{i} + n_y^\eta \mathbf{j} = \frac{1}{g^\eta} [-y \mathbf{i} + x \mathbf{j}] \quad (8b)$$

where $g^\xi = |\mathbf{g}^\xi| = \sqrt{(y_{,\eta})^2 + (-x_{,\eta})^2}$ and

$$g^\eta = |\mathbf{g}^\eta| = \sqrt{(-y)^2 + (x)^2}$$

Substituting the derivative relationships results in :

$$\begin{Bmatrix} \partial \\ \partial\hat{x} \\ \partial\hat{y} \end{Bmatrix} = \frac{1}{|\mathbf{J}|} \begin{bmatrix} g^\xi n_x^\xi \frac{\partial}{\partial\xi} & \frac{1}{\xi} g^\eta n_x^\eta \frac{\partial}{\partial\eta} \\ g^\xi n_y^\xi \frac{\partial}{\partial\xi} & \frac{1}{\xi} g^\eta n_y^\eta \frac{\partial}{\partial\eta} \end{bmatrix} \quad (9)$$

Substituting equation (9) into the differential operator $[\mathbf{L}]$ in equation (2) results in equation (10).

$$\begin{aligned} [\mathbf{L}] &= \frac{g^\xi}{|\mathbf{J}|} \begin{bmatrix} n_x^\xi & 0 \\ 0 & n_y^\xi \\ n_y^\xi & n_x^\xi \end{bmatrix} \frac{\partial}{\partial\xi} + \frac{g^\eta}{\xi |\mathbf{J}|} \begin{bmatrix} n_x^\eta & 0 \\ 0 & n_y^\eta \\ n_y^\eta & n_x^\eta \end{bmatrix} \frac{\partial}{\partial\eta} \\ &= [\mathbf{b}^1] \frac{\partial}{\partial\xi} + \frac{1}{\xi} [\mathbf{b}^2] \frac{\partial}{\partial\eta} \end{aligned} \quad (10)$$

where

$$[\mathbf{b}^1] = \frac{g^\xi}{|\mathbf{J}|} \begin{bmatrix} n_x^\xi & 0 \\ 0 & n_y^\xi \\ n_y^\xi & n_x^\xi \end{bmatrix} = \frac{1}{|\mathbf{J}|} \begin{bmatrix} y_{,\eta} & 0 \\ 0 & -x_{,\eta} \\ -x_{,\eta} & y_{,\eta} \end{bmatrix}$$

$$[\mathbf{b}^2] = \frac{g^\eta}{|\mathbf{J}|} \begin{bmatrix} n_x^\eta & 0 \\ 0 & n_y^\eta \\ n_y^\eta & n_x^\eta \end{bmatrix} = \frac{1}{|\mathbf{J}|} \begin{bmatrix} -y & 0 \\ 0 & x \\ x & -y \end{bmatrix}$$

Applying the transformation in equation (9) to the differential motion and continuity equations yields

$$\begin{aligned} & [b^1]^T \{\sigma'_{,\xi}\} + \frac{1}{\xi} [b^2]^T \{\sigma'_{,\eta}\} + [b^1]^T \{m\} p_{,\xi} \\ & + \frac{1}{\xi} [b^2]^T \{m\} p_{,\eta} + \omega^2 \rho \{u\} + \rho \{b\} = 0 \end{aligned} \quad (11)$$

$$\begin{aligned} & -k \{m\}^T \left([b^1] \frac{\partial}{\partial \xi} \left([b^1]^T \frac{\partial}{\partial \xi} + \frac{1}{\xi} [b^2]^T \frac{\partial}{\partial \eta} \right) \right. \\ & + \left. \frac{1}{\xi} [b^2] \frac{\partial}{\partial \eta} \left([b^1]^T \frac{\partial}{\partial \xi} + \frac{1}{\xi} [b^2]^T \frac{\partial}{\partial \eta} \right) \right) \{m\} p \\ & + \omega^2 k \rho_f \{m\}^T \left([b^1] \{u_{,\xi}\} + \frac{1}{\xi} [b^2] \{u_{,\eta}\} \right) \\ & + k \rho_f \{m\}^T \left([b^1] \{b_{,\xi}\} + \frac{1}{\xi} [b^2] \{b_{,\eta}\} \right) \\ & + i \omega \{m\}^T \left([b^1] \{u_{,\xi}\} + \frac{1}{\xi} [b^2] \{u_{,\eta}\} \right) + i \omega \frac{n}{K_f} p = 0 \end{aligned} \quad (12)$$

4 Displacements and pore pressure shape functions

Shape functions similar to the mapping interpolation functions may be used to interpolate the finite element displacements for all lines with constant ξ .

Using displacement shape functions $[N^u(\eta)]$ and displacements functions in the radial direction $\{u(\xi)\}$, the finite element displacement function may be represented as

$$\{u\} = \{u(\xi, \eta, \zeta)\} = [N^u] \{u(\xi)\} \quad (13a)$$

where $[N^u] = [N^u(\eta, \zeta)]$

and hence

$$\begin{aligned} \{u_{,\xi}\} &= [N^u]_{,\xi} \{u(\xi)\}_{,\xi}, \\ \{u_{,\eta}\} &= [N^u]_{,\eta} \{u(\xi)\}, \\ \{u_{,\zeta}\} &= [N^u]_{,\zeta} \{u(\xi)\} \end{aligned} \quad (13b)$$

Similarly, the pore pressure function may be represented using the shape functions $[N^p(\eta, \zeta)]$ and pressure functions in the radial direction $\{p(\xi)\}$. Hence the finite element pore pressure function may be represented as

$$p = \{p(\xi, \eta)\} [N^p] \{p(\xi)\} \quad (14a)$$

where $[N^p] = [N^p(\eta)]$

$$\text{and hence } p_{,\xi} = [N^p]_{,\xi} \{p(\xi)\}_{,\xi} \quad (14b)$$

$$p_{,\eta} = [N^p]_{,\eta} \{p(\xi)\},$$

$$p_{,\xi\xi} = [N^p]_{,\xi\xi} \{p(\xi)\}_{,\xi\xi},$$

where $p_{,\eta\eta} = [N^p]_{,\eta\eta} \{p(\xi)\}$ and

$$p_{,\xi\eta} = p_{,\eta\xi} = [N^p]_{,\eta\xi} \{p(\xi)\}_{,\xi}$$

The stresses, strains and displacements are related by

$$\{\sigma'\} = [D] \{\varepsilon\} = [D][L] \{u\} = [D][L][N^u] \{u(\xi)\} \quad (15)$$

where $[D]$ is the constitutive matrix and $[L] = [b^1] \frac{\partial}{\partial \xi} + \frac{1}{\xi} [b^2] \frac{\partial}{\partial \eta} + \frac{1}{\xi} [b^3] \frac{\partial}{\partial \zeta}$. This leads to

$$\begin{aligned} \{\sigma'\} &= [D] \left([b^1] \{u_{,\xi}\} + \frac{1}{\xi} [b^2] \{u_{,\eta}\} + \frac{1}{\xi} [b^3] \{u_{,\zeta}\} \right) \\ &= [D] \left([b^1] [N^u]_{,\xi} \{u(\xi)\}_{,\xi} \right. \\ & \quad \left. + \frac{1}{\xi} \left([b^2] [N^u]_{,\eta} + [b^3] [N^u]_{,\zeta} \right) \{u(\xi)\} \right) \end{aligned} \quad (16)$$

which can be expressed as

$$\{\sigma'\} = [D] \left([B_u^1] \{u(\xi)\}_{,\xi} + \frac{1}{\xi} [B_u^2] \{u(\xi)\} \right) \quad (17)$$

where $[B_u^1] = [b^1] [N^u(\eta)]_{,\xi} = [b^1] [N^u]_{,\xi}$ and $[B_u^2] = [b^2] [N^u(\eta)]_{,\eta} + [b^3] [N^u]_{,\zeta}$.

Note that $[B_u^1]$ and $[B_u^2]$ are not dependent on ξ , and hence differentiating $\{\sigma'\}$ leads to

$$\{\sigma'_{,\xi}\} = [D] \left([B_u^1] \{u(\xi)\}_{,\xi\xi} + \frac{1}{\xi} [B_u^2] \{u(\xi)\}_{,\xi} - \frac{1}{\xi^2} [B_u^2] \{u(\xi)\} \right) \quad (18)$$

5 Weighted-Residual Finite Element Approximation

To derive the finite element approximation, the Galerkin's weighted-residual method is applied to the transformed differential equations of motion and continuity, equations (11) and (12), by multiplying them with a weighting function $\{w\}^T = \{w(\xi, \eta)\}^T$ and then integrating over the domain A . Integration is from -1 to $+1$ for the boundary variable η while the integration in the ξ direction is from 0 to $+1$ for bounded elements and from $+1$ to ∞ for unbounded elements.

The weighting function $\{w^u\}^T$ to be multiplied by the differential equation of motion can be represented by the same displacement function as $\{w^u\} = \{w^u(\xi, \eta)\} = [N^u(\eta)]\{w^u(\xi)\}$. The weighting function $\{w^p\}^T$ to be multiplied by the differential equation of continuity, in turn, can be represented by the same pore pressure function as $\{w^p\} = \{w^p(\xi, \eta)\} = [N^p(\eta)]\{w^p(\xi)\}$. Green's theorem is finally applied to the line integral. The final equations are shown in Section 6.

6 Summary of the Finite Element Coupled Consolidation Equations

Due to the space restrictions, only the final formulation of the finite element derivation is presented in the form of the following equations.

$$\begin{aligned}
 & [E^0] \xi^2 \{u(\xi)\}_{,\xi\xi} + ([E^0] - [E^1] + [E^1]^T) \xi \{u(\xi)\}_{,\xi} \\
 & - [E^2] \{u(\xi)\} + \omega^2 [M^0] \xi^2 \{u(\xi)\} + [E^3] \xi^2 \{p(\xi)\}_{,\xi} \\
 & + ([E^3] - [E^4]) \xi \{p(\xi)\} + \xi^2 \{F^b(\xi)\} + \xi \{F^t(\xi)\} = 0
 \end{aligned}
 \tag{19}$$

$$\begin{aligned}
 & [E^5] \xi^2 \{p(\xi)\}_{,\xi\xi} + ([E^5] - [E^6] + [E^6]^T \\
 & + \{F^{t1}\}) \xi \{p(\xi)\}_{,\xi} + (-[E^7] + \{F^{t2}\}) \{p(\xi)\} \\
 & - i\omega [M^1] \xi^2 \{p(\xi)\} - (i\omega + \omega^2 k \rho_f) [E^3]^T \xi^2 \{u(\xi)\}_{,\xi} \\
 & - (i\omega + \omega^2 k \rho_f) ([E^3]^T - [E^{4p}] + \{F^{t3}\}) \xi \{u(\xi)\} \\
 & - k \rho_f (\xi^2 \{F^{b1}(\xi)\} + \xi \{F^{b2}(\xi)\} \\
 & - \xi \{F^{b3}(\xi)\} + \xi \{F^{b4}(\xi)\}) = 0
 \end{aligned}
 \tag{20}$$

Where

$$\begin{aligned}
 [E^0] &= \int_{-1}^{+1} [B_u^1]^T [D] [B_u^1] J |d\eta \\
 [E^1] &= \int_{-1}^{+1} [B_u^2]^T [D] [B_u^1] J |d\eta \\
 [E^2] &= \int_{-1}^{+1} [B_u^2]^T [D] [B_u^2] J |d\eta \\
 [E^3] &= \int_{-1}^{+1} [B_u^1]^T \{m\} [N^p] J |d\eta \\
 [E^4] &= \int_{-1}^{+1} [B_u^2]^T \{m\} [N^p] J |d\eta \\
 [E^{4p}] &= \int_{-1}^{+1} [B_p^2]^T [N^u] J |d\eta \\
 [E^5] &= \int_{-1}^{+1} [B_p^1]^T k [B_p^1] J |d\eta \\
 [E^6] &= \int_{-1}^{+1} [B_p^2]^T k [B_p^1] J |d\eta \\
 [E^7] &= \int_{-1}^{+1} [B_p^2]^T k [B_p^2] J |d\eta \\
 [M^0] &= \int_{-1}^{+1} [N^u]^T \rho [N^u] J |d\eta \\
 [M^1] &= \int_{-1}^{+1} [N^p]^T \frac{n}{K_f} [N^p] J |d\eta \\
 \{F^b(\xi)\} &= \int_{-1}^{+1} [N^u]^T \rho \{b\} J |d\eta \\
 \{F^t(\xi)\} &= \left([N^u]^T \{t^\eta(\xi)\} g^\eta \right)_{-1}^{+1} \\
 \{F^{t1}\} &= \left([B_p^{2A}]^T k [B_p^1] J \right)_{-1}^{+1} \\
 \{F^{t2}\} &= \left([B_p^{2A}]^T k [B_p^2] J \right)_{-1}^{+1} \\
 \{F^{t3}\} &= \left([B_p^{2A}]^T [N^u] J \right)_{-1}^{+1} \\
 \{F^{b1}(\xi)\} &= \int_{-1}^{+1} [B_p^1]^T \{b_{,\xi}\} J |d\eta \\
 \{F^{b2}(\xi)\} &= \int_{-1}^{+1} [B_p^1]^T \{b\} J |d\eta \\
 \{F^{b3}(\xi)\} &= \int_{-1}^{+1} [B_p^2]^T \{b\} J |d\eta
 \end{aligned}$$

$$\begin{aligned} \{F^{b^4}(\xi)\} &= \left([B_p^{2A}]^T \{b\} J \right)_{-1}^{+1} \\ [B_u^1] &= [b^1] [N^u(\eta)] = [b^1] [N^u] \\ [B_u^2] &= [b^2] [N^u(\eta)]_{,\eta} = [b^2] [N^u]_{,\eta} \\ [B_p^1] &= [b^1]^T \{m\} [N^p(\eta)] = [b^1]^T \{m\} [N^p] \\ [B_p^2] &= [b^2]^T \{m\} [N^p(\eta)]_{,\eta} = [b^2]^T \{m\} [N^p]_{,\eta} \\ [B_p^{2A}]^T &= [N^p(\eta)]^T \{m\}^T [b^2] = [N^p]^T \{m\}^T [b^2] \end{aligned}$$

Which have to be solved subject to the following boundary conditions;

$$\text{at } -1 \leq \eta < 1 \text{ and } \xi = 1 \quad \{u\} = \{c_1\}, \quad \{p\} = \{c_2\} \quad (21a)$$

$$\text{at } \eta = 1 \text{ and } 1 < \xi \leq \infty \quad \{p\} = 0 \quad (21b)$$

$$\text{at } -1 \leq \eta < 1 \text{ and } \xi = \infty \quad \{u\} = \{u_{,\xi}\} = \{p_{,\xi}\} = 0 \quad (21c)$$

Where $\{c_2\}$ and $\{c_2\}$ are constants. Full derivation of the above formulation is covered by Hassanen et al. [24].

7 Proposal for Solving the FE Coupled Consolidation Equations

The system of equations (19) and (20), subject to the boundary conditions (21 a, b, c), are $2n$ second order, non-homogenous and non-linear ordinary differential equations with constant coefficients, independent variable ξ and two unknowns u and p .

In the static load case, i.e. $\omega = 0$, the differential equation (20) contains $p(\xi)$ only. Therefore, the analytical solutions for both differential equations involving power functions in ξ permit the boundary condition at infinity ($\xi \rightarrow \infty$), finite p and finite u , to be satisfied exactly [25, 26, 27]. However, the analytical solution of full equations (19) and (20), subject to the boundary conditions (21 a, b, c), is not

available because the dynamic load, i.e. $\omega \neq 0$, is considered.

These equations can be numerically solved by finite difference or Chebyshev pseudospectral, as one of the spectral methods. On increasing n the interval h between grid points becomes smaller. This would cause the error to rapidly decrease even if the order of the method were fixed. For example, when h increases from 10 to 20, the error becomes $O(h^{20})$ in terms of the new, smaller h . Since h is $O(\frac{1}{n})$, we have

$$\text{Pseudospectral error} \approx O\left[\left(\frac{1}{n}\right)^n\right] \quad (22)$$

Therefore, the error is decreasing faster than any finite power of n because the power in the error formula is always increasing, too. This is infinite order or exponential convergence [28]. Therefore, when many decimal places of accuracy are needed, the contest between pseudospectral algorithms and finite difference is not an even battle but a rout: pseudospectral methods win hands-down. Moreover, engineers and mathematicians who need accurate many decimal places have always preferred spectral methods [28]. To decrease the error in equation (22), especially on increasing n or number of equations, Elbarbary and El-Sayed [29] has recently introduced a new pseudospectral differentiation matrix. Hence, on solving the second order differential equations (19) and (20) the error becomes nearly zero. The suggested proposal in the current section is being studied at the moment.

References:

- [1] Ch. Song and J.P. Wolf, Consistent infinitesimal finite-element-cell method: out-of-plane motion. The scaled boundary finite-element in the frequency domain, ASCE Journal of Engineering Mechanics, 121 (1995) 613-619.
- [2] J.P. Wolf and Ch. Song, Consistent infinitesimal finite element cell method: three dimensional vector wave equation, Int. J. Numer. Math. Eng. 39 (1996) 2189-2208.
- [3] Ch. Song and J.P. Wolf, The scaled boundary finite-element in the frequency domain, Comp. Meth. Appl. Mech. Engng., 164 (1998) 249-264.
- [4] Ch. Song and J.P. Wolf, The scaled boundary finite-element method alias consistent infinitesimal finite element cell method - for

- diffusion, *Int. J. Numer. Meth. Engng.* 45 (1999) 1403-1431.
- [5] J.P. Wolf and Ch. Song, The scaled boundary finite-element method a primer: derivation, *Comput. Struct.* 78 (2000) 191-210.
- [6] J.P. Wolf and Ch. Song, The scaled boundary finite-element method a fundamental solution less boundary-element method, *Comp. Meth. Appl. Mech. Engng.* 190 (2001) 5551-5568.
- [7] Z. Yang, Fully automatic modelling of mixed-mode crack propagation using scaled boundary finite element method, *Engineering Fracture Mechanics* (published online, 2006).
- [8] B. Li, L. Cheng and A.J. Deeks, Wave diffraction by vertical cylinder using the scaled boundary finite-element, *Proceedings CDROM of the sixth world congress on computational mechanics in conjunction with the second AsianPacific congress on computational mechanics.* Beijing, China; 2004.
- [9] B. Li, L. Cheng, A.J. Deeks and K.M. Zhao, Substructuring in the scaled boundary finite element analysis of wave diffraction. Research report no. C: 1858, School of Civil and Research Engineering, The University of Western Australia; 2004.
- [10] A.J. Deeks and J.P. Wolf, A virtual work derivation of the scaled boundary finite-element method for elastostatics, *Comput. Mech.* 28 (2002) 489-504.
- [11] A.J. Deeks and J.P. Wolf, Stress recovery and error estimation for the scaled boundary finite-element method, *Int. J. Numer. Meth. Engng.* 54 (2002) 557-83.
- [12] A.J. Deeks and J.P. Wolf, An h-hierarchical adaptive procedure for the scaled boundary finite-element method, *Int. J Numer. Meth. Engng.* 54 (2002) 585-605.
- [13] J.P. Wolf, *The Scaled Boundary Finite Element Method*, John Wiley and Sons, Chichester (2003).
- [14] A.J. Deeks and L. Cheng, Potential flow around obstacles using the scaled boundary finite element method, *Int. J. Numer. Methods Fluids* 41 (2003) 721-41.
- [15] B. Li, L. Cheng, A.J. Deeks and B. Teng, A modified scaled boundary finite-element method for problems with parallel side-faces. I. Theoretical developments, *Applied Ocean Research* (published online, 2006).
- [16] B. Li, L. Cheng, A.J. Deeks and B. Teng, A modified scaled boundary finite-element method for problems with parallel side-faces. II. Application and evaluation, *Applied Ocean Research* (published online, 2006).
- [17] T. Ekevid and N-E. Wiberg, Wave propagation related to high-speed train. A scaled boundary FE-approach for unbounded domains, *Comput. Methods Appl. Mech. Engng.* (2002) 191 3947-2964.
- [18] J.P. Wolf and Ch. Song, *Finite-Element Modelling of Unbounded Media*, John Wiley and Sons, Chichester (1996).
- [19] J.P. Doherty and A.J. Deeks, Adaptive coupling of the finite-element and scaled boundary finite-element methods for non-linear analysis of unbounded media, *Computers and Geotechnics* 32 (2005) 436-444.
- [20] J.P. Doherty and A.J. Deeks, Scaled boundary finite-element analysis of a non-homogeneous half-space, *Int. J. Numer. Meth. Engng.* 57 (2003) 955-973.
- [21] J.P. Doherty and A.J. Deeks, Scaled boundary finite-element analysis of a non-homogeneous axisymmetric domain subjected to general loading, *Int. J. Num. Anal. Meth. GeoMech.* 27 (2003) 813-835.
- [22] J.P. Doherty and A.J. Deeks, Elastic response of circular footings embedded in a non homogeneous half-space, *Geotechnique* 53 (2003) 703-714.
- [23] M.A. Biot, General theory of three-dimensional consolidation, *J. Appl. Phys.* 12 (1941) 155-164.
- [24] Hassanen M. and El-Hamalawi A. "Two-dimensional development of the dynamic coupled consolidation scaled boundary finite-element method for fully saturated soils" *Soil Dynamics and Earthquake Engineering*, Volume 27, Issue 2, 2007, Pages 153-165.
- [25] Ch. Song and J.P. Wolf, The scaled boundary finite-element method: analytical solution in frequency domain, *Comput. Methods Appl. Mech. Engng* 164 (1998) 249-264.
- [26] Ch. Song and J.P. Wolf, Body loads in scaled boundary finite-element method, *Comput. Methods Appl. Mech. Engng* 180 (1999) 117-135.
- [27] J.P. Wolf and F.G. Huot, On modelling unbounded saturated poroelastic soil with the scaled boundary finite-element method, *APCOM'01, First Asian-Pacific Congress on Computational Mechanics*, November 20-23, 2001, Sydney, Australia.
- [28] J.P. Boyd, *Chebyshev and Fourier Spectral Methods*, Dover, New York (2000).
- [29] E.M.E. Elbarbary and S. M. El-Sayed, Higher order pseudospectral differentiation matrices, *Applied Numerical Mathematics* 55 (2005) 425-438.